




Article

Opportunities and Limits of Using Meteorological Reanalysis Data for Simulating Seasonal to Sub-Daily Water Temperature Dynamics in a Large Shallow Lake

Marieke A. Frassl ^{1,2,*} , Bertram Boehrer ¹, Peter L. Holtermann ³, Weiping Hu ⁴,
Knut Klingbeil ^{3,5}, Zhaoliang Peng ⁴, Jinge Zhu ⁴ and Karsten Rinke ¹

¹ UFZ, Helmholtz Centre for Environmental Research, Department of Lake Research, Brückstraße 3 a, D-39114 Magdeburg, Germany; bertram.boehrer@ufz.de (B.B.); karsten.rinke@ufz.de (K.R.)

² Australian Rivers Institute, Griffith University, 170 Kessels Rd, Nathan, QLD 4111, Australia

³ Leibniz Institute for Baltic Sea Research, Seestraße 15, D-18119 Rostock-Warnemünde, Germany; peter.holtermann@io-warnemuende.de (P.L.H.); knut.klingbeil@io-warnemuende.de (K.K.)

⁴ State Key Laboratory of Lake Science and Environment, Nanjing Institute of Geography and Limnology, Chinese Academy of Sciences, Nanjing 210008, China; wp@niglas.ac.cn (W.H.); zlpeng@niglas.ac.cn (Z.P.); jgzhu@niglas.ac.cn (J.Z.)

⁵ Department of Mathematics, University of Hamburg, Bundesstraße 55, D-20146 Hamburg, Germany

* Correspondence: marieke.frassl@ufz.de or m.frassl@griffith.edu.au; Tel.: +61-7-3735-9225

Received: 4 March 2018; Accepted: 1 May 2018; Published: 3 May 2018



Abstract: In lakes and reservoirs, physical processes control temperature dynamics and stratification, which are important determinants of water quality. In large lakes, even extensive monitoring programs leave some of the patterns undiscovered and unresolved. Lake models can complement measurements in higher spatial and temporal resolution. These models require a set of driving data, particularly meteorological input data, which are compulsory to the models but at many locations not available at the desired scale or quality. It remains an open question whether these meteorological input data can be acquired in a sufficient quality by employing atmospheric models. In this study, we used the European Centre for Medium-Range Weather Forecasts' (ECMWF) ERA-Interim atmospheric reanalysis data as meteorological forcing for the three-dimensional hydrodynamic General Estuarine Transport Model (GETM). With this combination, we modelled the spatio-temporal variation in water temperature in the large, shallow Lake Chaohu, China. The model succeeded in reproducing the seasonal patterns of cooling and warming. While the model did predict diurnal patterns, these patterns were not precise enough to correctly estimate the extent of short stratification events. Nevertheless, applying reanalysis data proved useful for simulating general patterns of stratification dynamics and seasonal thermodynamics in a large shallow lake over the year. Utilising reanalysis data together with hydrodynamic models can, therefore, inform about water temperature dynamics in the respective water bodies and, by that, complement local measurements.

Keywords: GETM; Lake Chaohu; ERA-Interim; three-dimensional hydrodynamic modelling; stratification

1. Introduction

Shallow lakes are widely distributed across the globe [1], which is reflected in the low global average depths of 3.5 m for lakes in the smallest size class of 0.1–1 km² and generally low average depths across different continents [2]. Given their low average water depth, the water column of shallow lakes heats up faster compared to a deeper lake with the same surface area in the same climatic region [3,4]. This results in both larger diurnal temperature fluctuations as well as larger seasonal temperature ranges in shallow lakes. The morphological characteristics make shallow lakes

generally more susceptible to atmospheric forcing like irradiance, air temperature and wind friction [5]. This does not only refer to variables related to hydro- and thermodynamics but also affects water quality variables. For example, higher water temperatures combined with high nutrient concentrations lead to the frequent occurrence of persistent cyanobacteria blooms [6,7]. Usually, surface scums of cyanobacteria are not distributed homogeneously, but are constantly transported by wind and occur at a spatially-variable severity (e.g., [8]). This can result in larger horizontal than vertical gradients in shallow lakes [9,10]. Pronounced spatial patterns also have been observed for the occurrence of hypoxic zones, which lead to the dissolution of reduced metals and, thus, water quality deterioration (e.g., [11,12]).

This spatial variability, which is primarily caused by hydrodynamics, is difficult to cover through observations alone: ground-based measurements by moorings or ship-based measurements cannot be implemented in the required spatial and temporal resolution. While remote sensing develops into a promising technology to support the monitoring of lake surfaces (see the reviews by [13,14], the special issues [15,16] and the overview by [17]), it does not resolve the vertical dimension in the water column. In order to complement local measurements and to expand information along spatial and temporal scales, numerical models have been proven useful [18]. Depending on the question, they can be designed from one-dimensional models that resolve the vertical dimension to rather complex three-dimensional models. The latter have the benefit that they resolve both horizontal and vertical heterogeneity, as well as three-dimensional circulation patterns.

In oceanography, three-dimensional models have a long history of application (see e.g., [19]). They became more popular in limnological studies in the early 2000s [20–22] and are now used frequently to understand physical (e.g., [23,24]) and biological (e.g., [25,26]) processes in lakes and to assess the effects of lake management on oxic conditions [27] or phytoplankton dynamics [28]. In shallow lakes, three-dimensional models are commonly applied to analyze the occurrence of anoxia [29], resuspension events [30], cyanobacteria blooms [31] and to support management, e.g., by identifying critical nutrient loads [32,33]. Lake Taihu, a shallow lake similar to Lake Chaohu, has a long history of three-dimensional model applications (for an overview, see [34]). Three-dimensional lake models have the advantage being able to resolve most physical processes in the water body, e.g., long internal waves, upwelling and to analyse spatial phenomena like the distribution of surface scums (e.g., [35]) or the flux of nutrients through the benthic boundary layer [20,36] under pre-defined conditions. One open-source and publicly available three-dimensional hydrodynamic model is the General Estuarine Transport Model (GETM). GETM was originally developed for coastal ocean applications (see the review by [37]), but was also successfully applied to lakes (e.g., [38,39]). Important features for lake modelling are adaptive terrain-following coordinates [40]. This facilitates a proper vertical resolution of boundary layers. Within GETM, non-hydrostatic effects [41], which are required for high-resolution studies, can optionally be included. State-of-the-art vertical turbulence closure is provided via an interface to the General Ocean Turbulence Model (GOTM; [42]).

Three-dimensional models require a large amount of data for forcing and validation. In countries with a large territory or areas that are not easily accessible due to a lack of infrastructure (e.g., in some tropical countries or arctic regions), the high demand of input data is hard to satisfy since the necessary data to drive a complex model are in many cases not easily available at the required spatial and temporal resolution (e.g., [43]). Alternatively, local forcing data could be obtained from e.g., high-resolution atmospheric models (e.g., [44]). However, these local atmospheric models need to be nested into large-scale global models [45,46] or are often specific for a certain meteorological variable and developed for a specific region (e.g., [47]). The question arises, whether coarse meteorological and hydrological data from global models can be used directly for driving local lake models. This methodology would be easily transferable to other water bodies worldwide and would help to apply lake models in regions with scarce monitoring data.

Reanalysis projects assimilate weather forecast models with local observations leading to global datasets of atmospheric circulation [48]. The same data assimilation technique is applied over the

whole time period considered, resulting in a historically coherent dataset that is independent of methodological changes [48]. In addition, with the reanalysis approach being spatial, global coverage can be achieved [49]. The European Centre for Medium-Range Weather Forecasts (ECMWF, [48]) provides the ERA-Interim reanalysis consisting of a wide range of meteorological variables with a global coverage on a grid of 0.75 degrees (approx. 80 km) resolution. Only few lake-modelling studies have made use of reanalysis data. Layden et al. [50] used data from ERA-Interim to drive a global model application and estimate lake surface temperatures with the model FLake. Schmid et al. [51] used data from the NOAA NCEP-NCAR CDAS-1 reanalysis project to simulate CO₂ concentrations and temperature dynamics in a lake that is located in a data-scarce region. Piccolroaz and Toffolon made use of the consistency of reanalysis products and ran a long-term simulation for Lake Baikal [52]. Xue et al. [53] applied wind input from different sources as driving data for a three-dimensional model of Lake Superior. They found that wind input from a weather forecast model or from reanalysis data produced better modelling results than wind derived from local observations. This was due to the fact that spatial wind patterns, especially at the shore of the lake, were not captured by the observations [53].

In this study, we try to find an approach for modelling and analysing thermal and stratification dynamics in areas where only insufficient data is available. Sparse measurements often limit the validation of simulated overall circulation. This approach, therefore, requires some pragmatism in deriving information. It is our aim to explore the opportunities as well as the limits of using freely available reanalysis data for modelling seasonal to sub-daily temperature variability in large shallow lakes. The realistic reproduction of temperature dynamics and stratification periods is used as a criterion for evaluating the model performance. Analysing the hydrodynamic processes causing the stratification patterns remains out of the scope of the present study. As an exemplary test, we simulate the fifth-largest lake in China, Lake Chaohu, with the 3D hydrodynamic model GETM and spatially uniform atmospheric forcing extracted from the ERA-Interim reanalysis data set. We compare simulated with measured water temperatures at several locations within the lake over the course of one year.

2. Materials and Methods

2.1. Study Site

Lake Chaohu is located in the lower Yangtze River basin (31°43′–31°72′ N, 117°29′–117°85′ E, Figure 1). Its area covers 780 km² with a maximum length of 54.5 km from east to west and a maximum width of 21.0 km from south to north. Its average depth is approximately 3 m, and its maximum depth is 6 m [54]. Lake Chaohu is a major water body in the province of Anhui: the water of Lake Chaohu provides drinking water to approximately 250,000 people [55]. It serves for fisheries, transportation of goods, and as a recreational site. The two cities located at the shore of Lake Chaohu are Hefei in the west with approximately 7.6 million inhabitants [56] and Chaohu City in the east with approximately 1 million inhabitants [57].

Lake Chaohu is in a eutrophic state and each year from spring until late summer large cyanobacterial blooms develop in the lake and form surface scums, deteriorating the lake's water quality, leading to insecure drinking water supply and economic losses [58].

Lake Chaohu has 10 main tributaries that drain directly into the lake. Most of the inflows are located in the western part of the lake (Figure 1), and have small catchments and intermittent flows (for more information see Kong et al. [59]). Since the construction of a dam at the outflow in the eastern part of the lake in the early 1960s [59], the residence time in Lake Chaohu has varied between 160–210 days [59,60].

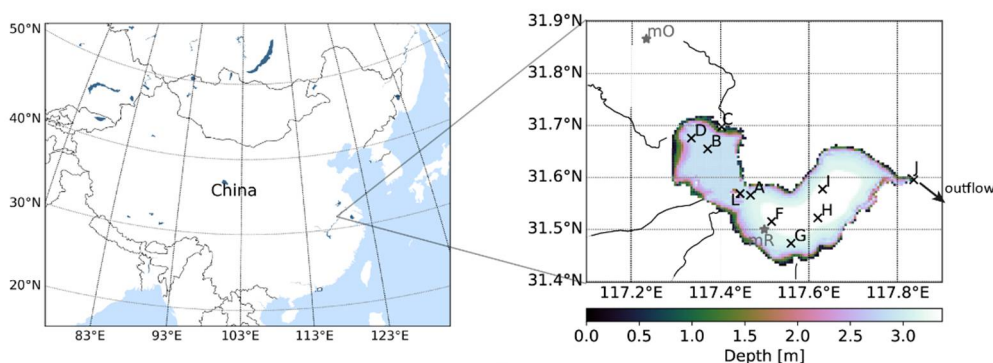


Figure 1. Location of Lake Chaohu in China (**left**) and model bathymetry for Lake Chaohu, including positions of the thermistor chains (**right**) and the main inflows; thermistor chain “E” and “K” are not shown because they were lost after a very short time of measurement and were not replaced; “mO” is the local meteorological station, “mR” is the grid point of the reanalysis; the outflow close to station J in the east of Lake Chaohu is regulated by a dam.

2.2. Lake Model

For the present study, we used the hydrostatic version of GETM to simulate Lake Chaohu on a spherical grid with approximately 500 m horizontal resolution. In the vertical, 7 terrain-following (sigma-) layers with a zooming towards the surface and bottom were utilised, resulting in a maximum layer thickness of 0.64 m. This provided sufficient vertical resolution to resolve the shear in boundary layers and the stratification throughout the water column, both required by GOTM to calculate vertical diffusivities from a well-calibrated k-epsilon closure. In order to support the accurate simulation of stratified water columns, the second-order TVD-Superbee scheme was used to reduce spurious numerical mixing of the thermocline [61]. Because of missing discharge data, the lake was treated as a closed basin of constant water volume. Heat loss through evaporation, however, was included in the simulation. We realised that this was a rather crude approximation, but it was our intention to follow a pragmatic approach that is easily applicable but also excluded uncertainties arising from poorly quantified or biased input data. A previous study by Chen and Liu [62] showed the limited influence of the inflows and the outflow on the whole lake thermodynamics and currents within the lake. In their modelling study, the outflow mainly influenced currents close to the dam in the eastern bay close to Chaohu City, while inflows had a negligible influence on the lake’s hydrodynamics. Another study by Huang et al. [60] found that wind had a larger effect on the lake’s hydrodynamics than changing in- and outflows. Additionally, while inflows could certainly affect nutrient dynamics in the lake, which were not considered here, its effect on thermodynamics and water temperatures would certainly be negligible, as energy exchange with the atmosphere had far more impact than energy exchange by in- and outflows.

For the calculation of longwave radiation, the equation of Idso and Jackson [63] was implemented into GETM. This equation had been used in other lake models (e.g., the General Lake Model (GLM; [64])) and showed a better model fit compared to a simulation with GETM’s standard equation by Clark, et al. [65] (see Table S1). Sensible and latent heat fluxes were calculated via bulk formulae according to Kondo [66].

Attenuation of shortwave radiation in the water column due to algal biomass and suspended matter was described by Jerlov coefficients that equal an extinction coefficient of 4.0 or an equivalent Secchi depth of about 0.36 m, which was the annual average in Lake Chaohu [67].

2.3. Atmospheric Forcing Data

Meteorological input data were obtained from the global reanalysis project ERA-Interim, developed and maintained by the European Centre for Medium-Range Weather Forecasts (ECMWF, [48]). Data were

downloaded from the public dataset web interface (<http://apps.ecmwf.int/datasets/>). ERA-Interim generates data with a resolution of 0.75 degrees (approximately 80 km horizontal resolution). Based on spatial interpolation, a resolution of 0.125 degrees (approximately 14 km horizontal resolution) is also available. These interpolated data allowed the derivation of the meteorological states at locations between the original grid nodes and permitted us to obtain data from one location in the center of the lake (31°30' N and 117°30' E). For this study, the provision of non-uniform meteorological input data was not considered appropriate because the comparatively coarse spatial resolution of ERA-Interim, compared to the dimensions of the lake (ca. 30 × 50 km), could not properly resolve the orographic features around the lake. Spatially heterogeneous meteorological input data would, thus, increase the complexity while introducing additional uncertainty, e.g., by neglecting the “urban heat island effect” [68] of the large cities Hefei and Chaohu City that are located in the west and east of the lake. We therefore decided to test the feasibility of a uniform atmospheric forcing and applied data from the single grid point over the whole model domain. The downloaded data included the variables air temperature (K), dewpoint temperature (K), 10 m U and V wind component (m s⁻¹), total cloud cover (-) and mean sea-level pressure (Pa). The data were available at 6-hourly time steps from the analysis (00:00, 06:00, 12:00 and 18:00) and 6-hourly time steps as forecast values (at 03:00, 09:00, 15:00 and 21:00), resulting in a temporal resolution of 3 h. Preceding the simulation, these meteorological data were linearly interpolated to hourly values. Air pressure values were taken as pressure at mean sea level, which complied with the low altitude of the lake of 8.4 m above sea level [59].

For a comparison of reanalysis data with locally measured data, daily averaged air temperature was downloaded from the NOAA data base (station Hefei, 31°52' N, 117°11' E; time period 2014–2016, [69]) and measured wind speed and direction were available from one station close to the lake (station Hefei, 31°52' N, 117°11' E) for part of the year 2015. Wind was measured at 10 m above ground, but gaps existed in the months May and August, and September was missing completely. Both air temperature and wind data were available at daily resolution.

Reanalysis data were compared to local measurements when available. For this comparative analysis, the downloaded reanalysis data, with the time step of 3 h, had to be averaged to daily data in order to achieve the same temporal resolution as the observed, daily averaged data.

2.4. In-Lake Measurements

From 1 November 2015 to 31 December 2016, thermistor chains were deployed and distributed evenly across the lake (Figure 1, Table S2). Stations K and L were deployed later in the project. Stations E and K (not shown in the map, Figure 1) were lost very soon after deployment and were not replaced. Data from these two stations were, therefore, not considered in our analyses. This led to a dataset of up to 10 locations at the same time. Each thermistor string consisted of three loggers (HOBO Onset[®], TidbiT; accuracy ±0.2 °C), located at a depth of 0.3 m below the surface as well as 0.2 and 1.5 m above the bottom. The measurement interval was set to 15 min. Due to the loss of loggers, large data gaps existed. However, missing loggers in the thermistor chain were replaced with new loggers as soon as possible; sometimes the whole thermistor chain had to be replaced. Due to the large data gaps, we focused most of our analysis on those stations that had surface and bottom temperatures available over several weeks at one time (stations A, B, D, F and J).

2.5. Analysis

The quality of the model results was quantified by calculating the Nash–Sutcliffe efficiency (*NSE*), the root mean square error (*RMSE*), and the mean absolute error (*MAE*), as:

$$NSE = 1 - \frac{\sum_{i=1}^n (y_i - \hat{y}_i)^2}{\sum_{i=1}^n (y_i - \bar{y})^2}, \quad (1)$$

$$RMSE = \sqrt{\frac{1}{n} \sum_{i=1}^n (y_i - \hat{y}_i)^2}, \quad (2)$$

$$MAE = \frac{1}{n} \sum_{i=1}^n |y_i - \hat{y}_i|, \quad (3)$$

where y_i was the observed, and \hat{y}_i the simulated water temperatures; \bar{y} was the mean observed water temperature at time i ; and n was the overall number of samples. Sub-daily temperature measurements at nine different locations in the lake were used for validation, because a good agreement between model and observation at different sites in the lake could only be reached by correctly simulating heat exchange across the surface as well as advection and diffusion within the lake.

Stratification duration in observed as well as simulated data was quantified by first calculating the temperature difference T_{diff} between surface and bottom temperature per station. We defined the water column as being stratified whenever this temperature difference surpassed 0.5 K (compare [70]). The stratification duration was then simply the accumulated time with T_{diff} above 0.5 K. We referred to the time between mixed conditions as a ‘stratification event’. The calculations were done for both observation and simulation only at times where both surface and bottom data were available from observations. Observations and simulation results were compared for stratification duration and for the amount of stratification events that lasted longer than 1 day.

3. Results

3.1. Meteorological Data

Reanalysis air temperatures (T_{rean}) matched well with observed ones (T_{obs}) (Figure 2, $T_{rean} = 0.98 \times T_{obs} + 0.54$, $r^2 = 0.9828$, p -value: <0.001). Wind speed from reanalysis data overestimated measured data on average by 0.27 m s^{-1} , i.e., 12%. Locally measured wind direction showed a higher variability than the reanalysed data. For the year 2015, reanalysis data showed the main wind direction from ENE, while local measurements did not display a main wind direction (Figure 2).

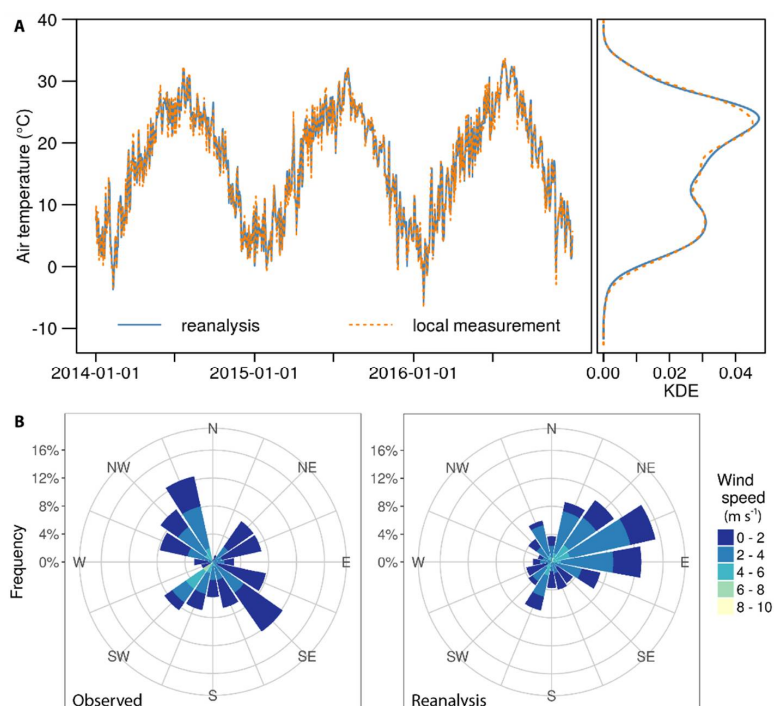


Figure 2. Comparison of local measurements (dotted orange) and reanalysis data (solid blue) of daily averaged air temperature, with data over time (panel A, left) and kernel density estimate (KDE; panel A, right). Comparison of daily averaged wind data from local observation (panel B, left) and reanalysis data (panel B, right); wind data were measured in 2015, except September. The different time periods were a consequence of data availability (compare Table S2).

3.2. Field Observations

The observed water temperatures followed the seasonal course in air temperatures (Figure 3). Over the whole measurement period water temperature ranged between 0.9 °C and 29.7 °C. It should be noted that no data were taken in midsummer, i.e., the maximum water temperature could be higher. Cooling and warming of the lake did not occur continuously. Instead, water temperature dropped or increased stepwise by several Kelvin over a few days (e.g., around day of the year 274 and day of the year 300, Figure 3 and 14th–18th of April, Figure 4). Exemplarily, the maximal gradients in the observation were a 3.2 K decrease over two days (1.6 K/day, station B, bottom, 8 March 2016), 4.1 K decrease over three days (1.4 K/day, station J, surface, 23 November 2015), and 7.0 K increase over 10 days (0.7 K/day, station B, 1.5 m above bottom, 3 February 2016).

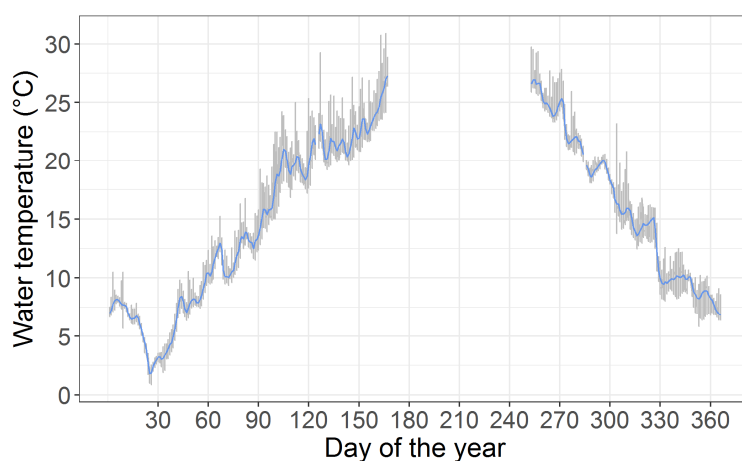


Figure 3. Measured water temperatures from the year 2016, the complete observation dataset is shown; blue: mean temperature per day of the year, grey: temperature range per day of the year. Temperature mean and range were calculated from all available data, i.e., each station and depth, for that day of the year.

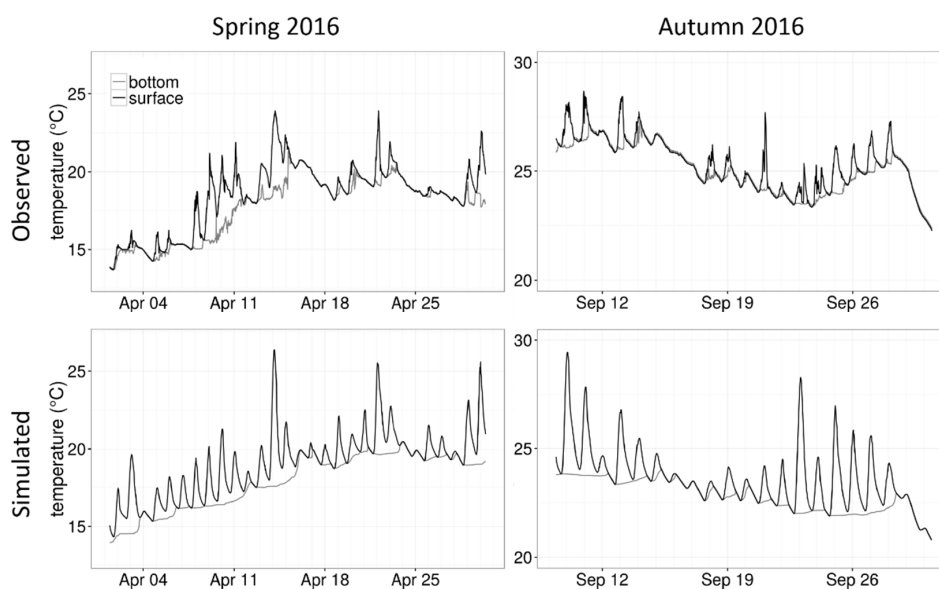


Figure 4. Water temperature in Lake Chaohu in spring 2016 (left) and autumn 2016 (right). Shown are measured data (top) and simulation results (bottom) of surface (black) and bottom water temperature (gray) at station F, which had both surface and bottom data available over a longer time period both in spring and autumn.

Although the lake is shallow, vertical stratification was observed, which could last for a few days (e.g., 8–11 April and 12–14 April, Figure 4, station F was chosen as an example since it had both surface and bottom data available over a longer period both in spring and in autumn). The maximum difference between bottom and surface temperature was observed at station B with 6.9 K at 9 April 2016. With a temperature range of up to 6.5 K, surface temperatures showed stronger daily fluctuations compared to bottom temperatures having a maximum daily temperature range of 3.7 K. During the year 2016, a maximum of 10 stratification events where the lake remained stratified for more than one day was observed at a single station (station D, Figure 5A). The longest observed stratification duration was 5.6 days (in April at station B). The median of the observed stratification duration was 3.5 h. Most observed stratification events had a short duration, i.e., 0.5–2 h (Figure 5B). During the time observed in the year 2016, the lake was stratified on average for 22% of all observations (30-min measurement interval, Table 1). Note that this number is relative to the available measurements and cannot be related to the whole year 2016. Large data gaps exist, especially in summer.

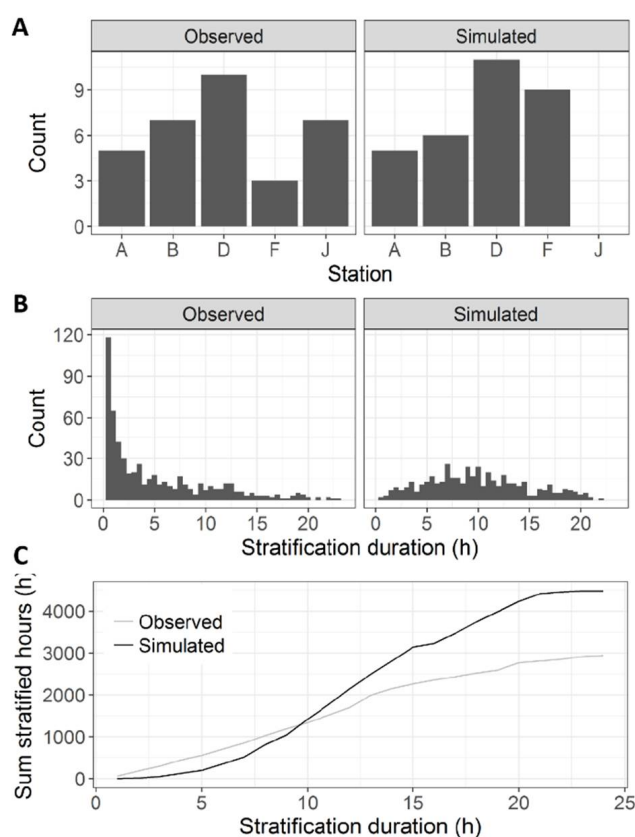


Figure 5. Amount of stratification events that lasted more than one day, differentiated by station and separated for observation (A, left) and simulation (A, right). Distribution of the length of stratification events lasting shorter than one day (B); cumulative sum of stratified time for those stratification events (C); for panel B and C data were taken from stations A, B, D, F and J. Note that the difference between stations in panel A can result from a different amount of data available from those stations.

Table 1. Overall duration of water temperature observations at different stations in Lake Chaohu; duration of stratified hours derived from observation and simulation; difference in prediction of stratified conditions. Data gaps exist and the numbers do not cover a complete year. The comparison below was done for those times when observations were available, i.e., only a subset of the simulation was taken into account.

Station	Total		Time Stratified				
	Observed	Observed	Simulated		Simulated–Observed		
	(h)	(h)	(%)	(h)	(%)	(h)	(%)
A	4685	648	13.83	1270	27.11	622	13.28
B	3565	924	25.92	1166	32.71	242	6.79
D	4572	1263	27.62	1783	39.00	520	11.37
F	3694	710	19.22	1702	46.07	992	26.85
J	4558	943	20.69	804	17.64	−139	−3.05
average	4215	898	21.46	1345	32.51	447	11.05

Most of the time observed, surface water temperatures differed between stations across the lake (Figure 6), demonstrating the heterogeneity of the water body in the horizontal direction. During the observation, horizontal temperature differences reached a maximum of 4.9 K at the surface, over a distance of 21.5 km between stations H and J and a maximal difference of 3.7 K at the bottom over a distance of 24.7 km between stations D and F.

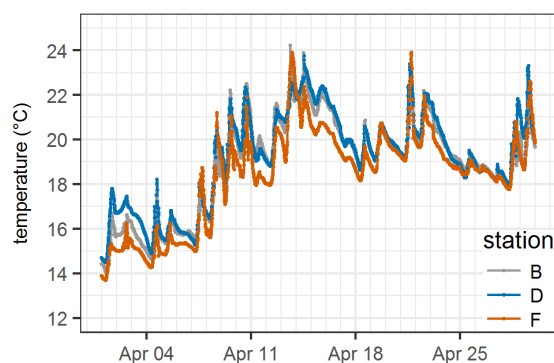


Figure 6. Observed surface water temperatures at stations B, D, F, zoomed to April 2016 to exemplarily visualize the horizontal differences.

3.3. Simulation Results

Overall, the simulation of water temperatures showed reasonable agreement with observations (Figure 7, Tables S1 and S3, Figures S1–S3). Surface temperatures were slightly underestimated in winter and overestimated in summer. In the months November and October 2016, simulated temperature was on average 1.6 K lower than the observed temperature. In June 2016 (the summer month with available data), simulated temperatures were on average 0.5 K higher compared to observed ones. This bias can also be seen from the linear regression for the complete simulation run (surface temperatures: $T_{\text{meas}} = 1.04 \times T_{\text{sim}} - 1.35$, $r^2 = 0.948$, $NSE = 0.92$, $RMSE = 1.61$, $MAE = 2.61$, $n = 71,541$, Table S1 and Figure S1). Bottom temperatures were generally slightly underestimated, on average 1.8 K in November–December 2016 and 0.3 K in June 2016 (bottom temperatures: $T_{\text{meas}} = 1.00 \times T_{\text{sim}} - 0.98$, $r^2 = 0.958$, $NSE = 0.93$, $RMSE = 1.64$, $MAE = 2.68$, $n = 75,669$, Table S1 and Figure S1).

The model reproduced the seasonal trend of surface and bottom temperature (Figures 7 and 8; here we exemplarily show station B, which had the least data gaps of all stations) as well as observed cooling events that lasted over a few days (Figure 8). Simulated temperatures showed diurnal stratification, too. However, the simulated stratification was more pronounced, occurred more

frequently, and showed a larger temperature difference between bottom and surface temperature compared to observations (Figure 4). While the amount of longer stratification events showed a good fit for the western part of the lake (Figure 5A, stations A, B and D), the fit was poor for the eastern part of the lake (Figure 5A, stations F and J). Combining information from all five stations, the simulated stratification duration lasted longer (Figure 5B) and thus did not show the high number of very short stratification events (0.5–4 h) as was observed (Figure 5B). Overall, the model overestimated the number of stratified hours in the lake by 11% (Figure 5C, Table 1). This comparison showed a good fit for stations B and J, whereas the weakest fit was obtained at station F (Table 1). This result is reflected in the model fits separated by station (Table S3), where the linear model for bottom temperatures at station F appeared to be not significant.

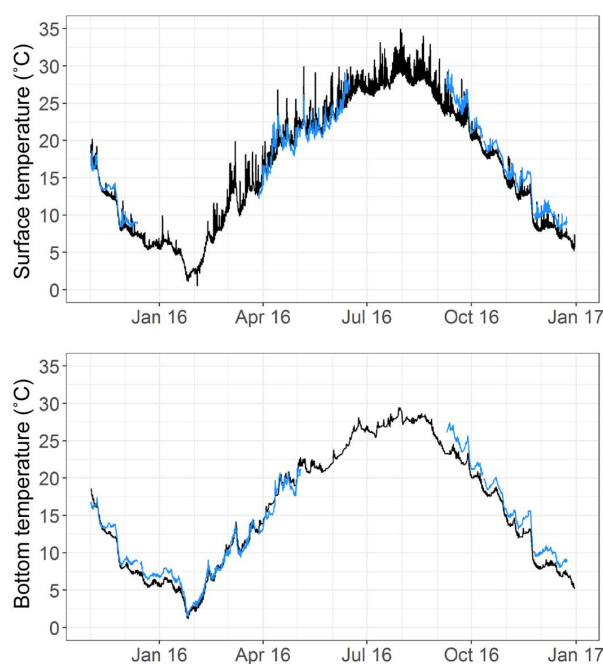


Figure 7. Water temperature, exemplarily shown at station B at the surface (**top**) and bottom (**bottom**). Blue: observations, black: simulation (the other stations are shown in the Supplements).

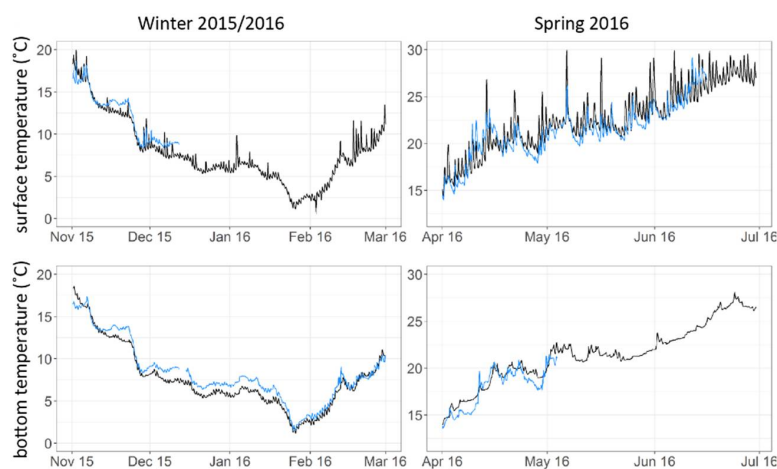


Figure 8. Seasonal cooling and warming events in Lake Chaohu in winter 2015/2016 (**left**) and spring 2016 (**right**). Shown is the water temperature exemplarily at station B at the surface (**top**) and bottom (**bottom**); blue: measurement, black: simulation.

4. Discussion

In this paper, a three-dimensional coastal ocean model was applied to simulate thermal and stratification dynamics of a large shallow lake in the Yangtze River basin in China. The model was driven by ERA-Interim reanalysis data. Measured by common model fit metrics (*NSE*, *RMSE*, *MAE*), the seasonal dynamics in surface and bottom temperature were reproduced well. The combination of data and model succeeded in reproducing synoptic-scale cooling and warming events. However, diurnal stratification patterns predicted by the model were too regular compared to that observed: stratification occurred more often in the model and, on average, lasted longer compared to observations.

Stratification in shallow lakes is heavily affected by wind and by heat fluxes at the water surface [71]. A comparison of wind data obtained from the reanalysis data and local measurements showed that wind speed was overestimated in the reanalysis data (0.27 m s^{-1} , i.e., 12%) and that wind directions diverged from each other. However, wind is unlikely to be responsible for the mismatch in stratification. Overestimations in wind speed would rather weaken instead of intensifying stratification in the model. Although wind directions in the reanalysis data differed from measured directions, they were similar to what has been denoted as the main wind direction in Chaohu by others [54,60,62]. Huang et al. [60] denote an eastern wind as the main wind direction between 2011 and 2013, which is comparable to the reanalysis from 2015 (Figure 2). Chen and Liu [62] state the main wind direction as south-east in summer. Dividing the reanalysis per month led to main wind directions either from south–south-west or east–north-east during the months June–August of the years 2014–2015 (data not shown). In winter, wind direction was more variable in the reanalysis with a stronger tendency towards the north-east as the main wind direction compared to the north-west stated as the main wind direction in winter by Chen and Liu [62]. In general, wind was found to be a meteorological variable that is well represented by reanalysis data [53] although the spatial resolution of the reanalysis does not account for local orography at small scale. It has to be noted that Xue et al. [53] used reanalysis data to simulate Lake Superior, which is more than 10 times the size of Lake Chaohu. Whether a bias in wind data from the reanalysis is causing the observed mismatch of longer stratification events in the eastern part of the lake (Figure 5A, stations F and J) can only be clarified through local measurements at various stations on and around the lake. The paper by Zhang et al. [54] hints at local differences in wind direction between Heifei and Chaohu City.

A difficulty in correctly simulating stratification in lakes arises from the surface-energy budget. Preliminary simulations revealed a high sensitivity of the model towards the equation used for calculating net longwave radiation fluxes. Furthermore, the model results showed a large diurnal fluctuation of surface water temperatures, which points to problems in the sub-daily energy budget. It is possible that cloud cover, which is part of the heat budget estimation, contributes a large error, since it is hard to simulate within global climate and forecast models [72].

A direct assessment of sub-daily patterns in reanalysis data could not be achieved since local measurements were only available as daily averages. Furthermore, it has to be kept in mind that local weather conditions can also be very heterogeneous around the lake leading to further complications. Daily land–lake wind patterns can develop due to different warming and cooling rates of land and water surfaces, and evaporation from the large surface area can have a buffering effect on local temperatures as well as changing local cloud cover and thus incoming irradiance. These processes are not included in the reanalysis model and would improve model performance [73].

Due to the unavailability of local data, we were not able to quantify the lake's water balance and neglected in- and outflows in our simulation. Our assumption is strengthened by previous simulation studies, which have shown the negligible effect of discharge on the lake's hydrodynamics [60,62]. We cannot completely exclude local effects of river inflows on stratification. An assessment of small-scale patterns would need reliable discharge data and several thermistor chains deployed close to the main inflows. Changes in water depth can potentially affect stratification. The water level in Lake Chaohu rises mainly in summer due to the rainy season (see e.g., [60]). If this had an effect, we would expect a strong seasonal bias in the model fit, which we did not observe. Other factors

that could contribute to the spatial mismatch of longer stratification events are potential errors in the bathymetry used for the simulations, the spatial resolution of the model, the operation of the dam, and even ship traffic. The lake is deeper in the eastern part. Inaccuracies in the bathymetry could have caused the mismatch at station F. Station J is located in a narrow bay, close to Chaohu City. A higher resolution of the model, as well as data on the dam operation could result in a better prediction at this location. Finally, Lake Chaohu is strongly used for the transportation of goods, leading to continuous ship traffic that causes turbulence in the water column. Station J could especially be affected by ship and boat traffic, since it is located in a bay of the lake, near to Chaohu City.

4.1. Applicability of Reanalysis Data in Hydrodynamic Lake Simulations

Within an initiative of the International Association of Hydrological Sciences (IAHS), the project Predictions in Ungauged Basins (PUB) was launched in 2003 (<http://iahs.info/pub/index.php>). PUB aimed at developing methods to increase the process-understanding and reduce the uncertainty of hydrological predictions in ungauged basins. The group mainly evolved from the need to develop models that are capable of providing reliable and transferable prognoses for future changes and for areas with little measurement activity [74]. Furthermore, new possibilities for data acquisition, e.g., remote sensing, were supposed to be explored [75]. In essence, the lake modelling community is confronted with similar problems: several surface water resources around the globe are at risk concerning water quality and quantity. Where standards in environmental monitoring are below the input data requirements of the established models, an alternative approach enabling model applications to those lakes and reservoirs is needed.

Despite the restrictions mentioned above, the model results described seasonal and synoptic scale patterns of water temperatures well, both at the surface and bottom of the lake. The lake morphometry prescribes a strong influence of meteorology on water temperature dynamics so that changes in meteorological conditions induce a fast thermodynamic response of the lake. Due to the shallow water depth, the effect of thermal inertia in spring and autumn, as observed in deep lakes with a large water volume, is strongly reduced. A potential buffering effect may arise from heat storage in the sediments or from groundwater intrusions leading to cooling in early summer and warming in autumn. Our simulated and observed temperature, however, did not provide evidence that such buffering effects are important in Lake Chaohu. Also, inflow and outflow dynamics of the lake are obviously negligible for the thermodynamic budget since our model was able to simulate temperature dynamics accurately without including in- and outflows. In conclusion, the direct effect of local meteorological conditions will be the main driver of the lake thermal and stratification dynamics. The good fit between observation and simulation regarding seasonal patterns showed that reanalysis data are suitable for simulations unless sub-daily dynamics are of interest. Our approach of applying reanalysis data has the benefits of easy transferability and the potential for global applicability since reanalysis data are available worldwide.

An important measure for water managers are the currents in the lake. An accumulation of cyanobacterial scums in the western part of the lake has been observed in several studies (e.g., [54,76,77]). It would be of interest to assess the feasibility of reanalysis data for simulating current patterns in lakes. However, we argue that a full assessment of currents in the lake requires local measurements for validation to give an indication on the reliability of those simulation results.

4.2. Water Temperature Data

Through our measurements of water temperatures at the surface and bottom of the lake, we showed that the large polymictic Lake Chaohu is frequently stratified. This contrasts with Huang et al. [60], who assumed that the lake does not stratify. We observed that the lake was stratified on average in 22% of all observations. It has to be stressed that this number does not relate to the whole year, since large data gaps exist in our dataset. It is probable that the percentage per year is higher, because the largest data gap existed in summer when the water column is most likely to stratify.

Stratification sometimes lasted over several days. As the lower layer of a stratified water body does not have direct contact with atmospheric oxygen, the huge oxygen demand of the sediment favors anoxic conditions in the bottom layer of the lake. The longer the stratification, the more likely the lake system develops anoxic bottom water. A precise simulation of stratification and the timing is, thus, mandatory for a realistic simulation of the bio-geochemistry of Lake Chaohu.

The frequent alteration between mixing and stratification could even increase the release of nutrients from the sediment to the overlying water. While the lake is stratified, nutrients may accumulate in the bottom layers. When the lake is mixed again, these nutrients will be diluted within the whole water column and can readily be taken up by primary producers. This “nutrient pump” can generate high pulses of nutrients, if the bottom waters approach anoxic conditions and low redox potentials persist [78]. In several studies, the occurrence of large anoxic zones, so called “black blooms”, in the shallow lakes of the Yangtze basin has been identified [12]. A three-dimensional modelling study would be useful for analysing hydrodynamic processes leading to these phenomena. However, this will require additional information from local meteorological and probably hydrological measurements in combination with a well calibrated bio-geochemical model. Coupling GETM to a biogeochemical model is straightforward via the Framework for Aquatic Biogeochemical Models (FABM; [79]). The limiting factor of such a study remains the availability of water quality data to validate the bio-geochemical model thoroughly.

Supplementary Materials: The following are available online at <http://www.mdpi.com/2073-4441/10/5/594/s1>, Table S1: Overall model fit. Figure S1: Model fit for the overall simulation. Table S2: Overview of data availability. Table S3: Model fit separated for stations. Figure S2: Water temperature at the surface. Figure S3: Water temperature at the bottom.

Author Contributions: M.F., B.B., W.H. and K.R. conceived and designed the study; M.F., P.H. and K.K. performed the modelling; M.F. analysed the data; W.H., Z.P. and J.Z. contributed data; M.F., K.K., Z.P. and K.R. wrote the first draft of the paper. All authors contributed in reviewing and editing the manuscript. Except for the lead-author and last author, authors are listed in alphabetic order.

Acknowledgments: Funding for this work was provided by the German Federal Ministry of Education and Research (BMBF) CLIENT program “International Partnerships for Sustainable Innovations” for the project “Managing Water Resources for Urban Catchments” (grant number 02WCL1337A) and by the German Academic Exchange Service (DAAD) under grant no. 57218695. Financial support of K. Klingbeil was provided by the Collaborative Research Center TRR181 on Energy Transfers in Atmosphere and Ocean. Reanalysis data were obtained from the ECMWF. Analysis, data-processing and generation of figures was done with the statistical software R (R Core Team, 2017 [80]; packages ncd4, tidyR and ggplot2) and the programming language Python (packages numpy, pylab, netCDF4 and seaborn). We thank two anonymous reviewers for their constructive comments to improve the quality of the manuscript.

Conflicts of Interest: The authors declare no conflict of interest.

References

1. Scheffer, M. *Ecology of Shallow Lakes*, 1st ed.; Kluwer Academic Publishers: Dordrecht, The Netherlands, 2004.
2. Messenger, M.L.; Lehner, B.; Grill, G.; Nedeva, I.; Schmitt, O. Estimating the volume and age of water stored in global lakes using a geo-statistical approach. *Nat. Commun.* **2016**, *7*, 1360. [[CrossRef](#)] [[PubMed](#)]
3. Toffolon, M.; Piccolroaz, S.; Majone, B.; Soja, A.; Peeters, F.; Schmid, M.; Wüest, A. Prediction of surface temperature in lakes with different morphology using air temperature. *Limnol. Oceanogr.* **2014**, *59*, 2185–2202. [[CrossRef](#)]
4. Woolway, R.I.; Jones, I.D.; Maberly, S.C.; French, J.R.; Livingstone, D.M.; Monteith, D.T.; Simpson, G.L.; Thackeray, S.J.; Andersen, M.R.; Battarbee, R.W.; et al. Diel Surface Temperature Range Scales with Lake Size. *PLoS ONE* **2016**, *11*. [[CrossRef](#)] [[PubMed](#)]
5. Woolway, R.I.; Meinson, P.; Nôges, P.; Jones, I.D.; Laas, A. Atmospheric stilling leads to prolonged thermal stratification in a large shallow polymictic lake. *Clim. Chang.* **2017**, *141*, 759–773. [[CrossRef](#)]
6. Hallegraeff, G.M. A review of harmful algal blooms and their apparent global increase. *Phycologia* **1993**, *32*, 79–99. [[CrossRef](#)]

7. Rigosi, A.; Carey, C.C.; Ibelings, B.W.; Brookes, J.D. The interaction between climate warming and eutrophication to promote cyanobacteria is dependent on trophic state and varies among taxa. *Limnol. Oceanogr.* **2014**, *59*, 99–114. [[CrossRef](#)]
8. Ibelings, B.W.V.M.; Los, H.F.J.; van der Molen, D.T.; Mooij, W.M. Fuzzy modeling of cyanobacterial surface waterblooms: Validation with NOAA-AVHRR satellite images. *Ecol. Appl.* **2003**, *13*, 1456–1472. [[CrossRef](#)]
9. De Souza Cardoso, L.; da Motta Marques, D. Hydrodynamics-driven plankton community in a shallow lake. *Aquat. Ecol.* **2007**, *43*, 73–84. [[CrossRef](#)]
10. Wang, C.; Feng, T.; Wang, P.; Hou, J.; Qian, J. Understanding the transport feature of bloom-forming *Microcystis* in a large shallow lake: A new combined hydrodynamic and spatially explicit agent-based modelling approach. *Ecol. Model.* **2017**, *343*, 25–38. [[CrossRef](#)]
11. Bocaniov, S.A.; Scavia, D. Temporal and spatial dynamics of large lake hypoxia: Integrating statistical and three-dimensional dynamic models to enhance lake management criteria. *Water Resour. Res.* **2016**, *52*, 4247–4263. [[CrossRef](#)]
12. Zhang, Y.; Shi, K.; Liu, J.; Deng, J.; Qin, B.; Zhu, G.; Zhou, Y. Meteorological and hydrological conditions driving the formation and disappearance of black blooms, an ecological disaster phenomena of eutrophication and algal blooms. *Sci. Total Environ.* **2016**, *569–570*, 1517–1529. [[CrossRef](#)] [[PubMed](#)]
13. Odermatt, D.; Gitelson, A.; Brando, V.E.; Schaepman, M. Review of constituent retrieval in optically deep and complex waters from satellite imagery. *Remote Sens. Environ.* **2012**, *118*, 116–126. [[CrossRef](#)]
14. Dörnhöfer, K.; Oppelt, N. Remote sensing for lake research and monitoring—Recent advances. *Ecol. Indic.* **2016**, *64*, 105–122. [[CrossRef](#)]
15. Zilioli, E. Preface. *Sci. Total Environ.* **2001**, *268*, 1–2. [[CrossRef](#)]
16. Palmer, S.C.; Kutser, T.; Hunter, P.D. Remote sensing of inland waters: Challenges, progress and future directions Remote Sensing of Environment. *Remote Sens. Environ.* **2015**, *157*, 1–8. [[CrossRef](#)]
17. Kwok, R. Ecology’s remote-sensing revolution. *Nature* **2018**, *556*, 137–138. [[CrossRef](#)] [[PubMed](#)]
18. Mooij, W.M.; Trolle, D.; Jeppesen, E.; Arhonditsis, G.; Belolipetsky, P.V.; Chitamwebwa, D.B.R.; Degermendzhy, A.G.; DeAngelis, D.L.; De Senerpont Domis, L.N.; Downing, A.S.; et al. Challenges and opportunities for integrating lake ecosystem modelling approaches. *Aquat. Ecol.* **2010**, *44*, 633–667. [[CrossRef](#)]
19. McWilliams, J.C. Modeling the oceanic general circulation. *Annu. Rev. Fluid Mech.* **1996**, *28*, 215–248. [[CrossRef](#)]
20. Hodges, B.R.; Imberger, J.; Saggio, A.; Winters, K.B. Modeling basin-scale internal waves in a stratified lake. *Limnol. Oceanogr.* **2000**, *45*, 1603–1620. [[CrossRef](#)]
21. Rueda, F.J.; Schladow, S.G. Quantitative Comparison of Models for Barotropic Response of Homogeneous Basins. *J. Hydraul. Eng.* **2002**, *128*, 201–213. [[CrossRef](#)]
22. Appt, J.; Imberger, J.; Kobus, H. Basin-scale motion in stratified Upper Lake Constance. *Limnol. Oceanogr.* **2004**, 919–933. [[CrossRef](#)]
23. Bocaniov, S.A.; Ullmann, C.; Rinke, K.; Lamb, K.G.; Boehrer, B. Internal waves and mixing in a stratified reservoir: Insights from three-dimensional modeling. *Limnologica* **2014**, *49*, 52–67. [[CrossRef](#)]
24. Valerio, G.; Cantelli, A.; Monti, P.; Leuzzi, G. A modeling approach to identify the effective forcing exerted by wind on a prealpine lake surrounded by a complex topography. *Water Resour. Res.* **2017**, *53*, 4036–4052. [[CrossRef](#)]
25. Missaghi, S.; Hondzo, M. Evaluation and application of a three-dimensional water quality model in a shallow lake with complex morphometry. *Ecol. Model.* **2010**, *221*, 1512–1525. [[CrossRef](#)]
26. Carraro, E.; Guyennon, N.; Hamilton, D.; Valsecchi, L.; Manfredi, E.C.; Viviano, G.; Salerno, F.; Tartari, G.; Copetti, D. Coupling high-resolution measurements to a three-dimensional lake model to assess the spatial and temporal dynamics of the cyanobacterium *Planktothrix rubescens* in a medium-sized lake. *Hydrobiologia* **2012**, *698*, 77–95. [[CrossRef](#)]
27. Toffolon, M.; Serafini, M. Effects of artificial hypolimnetic oxygenation in a shallow lake. Part 2: Numerical modelling. *J. Environ. Manag.* **2013**, *114*, 530–539. [[CrossRef](#)] [[PubMed](#)]
28. Chen, S.; Carey, C.C.; Little, J.C.; Lofton, M.E.; McClure, R.P.; Lei, C. Effectiveness of a bubble-plume mixing system for managing phytoplankton in lakes and reservoirs. *Ecol. Eng.* **2018**, *113*, 43–51. [[CrossRef](#)]
29. Leon, L.F.; Smith, R.E.; Romero, J.R.; Hecky, R.E. Lake Erie hypoxia simulations with ELCOM-CAEDYM. In Proceedings of the 3rd Biennial Meeting of the International Environmental Modelling and Software Society, Burlington, VT, USA, 9–13 July 2006.

30. Jin, K.-R.; Ji, Z.-G. Application and Validation of Three-Dimensional Model in a Shallow Lake. *J. Waterway Port Coast. Ocean Eng.* **2005**, *131*, 213–225. [[CrossRef](#)]
31. Li, W.; Qin, B.; Zhu, G. Forecasting short-term cyanobacterial blooms in Lake Taihu, China, using a coupled hydrodynamic–algal biomass model. *Ecohydrology* **2014**, *7*, 794–802. [[CrossRef](#)]
32. Tang, C.; Li, Y.; Acharya, K. Modeling the effects of external nutrient reductions on algal blooms in hyper-eutrophic Lake Taihu, China. *Ecol. Eng.* **2016**, *94*, 164–173. [[CrossRef](#)]
33. Janssen, A.B.; de Jager, V.C.; Janse, J.H.; Kong, X.; Liu, S.; Ye, Q.; Mooij, W.M. Spatial identification of critical nutrient loads of large shallow lakes: Implications for Lake Taihu (China). *Water Res.* **2017**, *119*, 276–287. [[CrossRef](#)] [[PubMed](#)]
34. Hu, W. A review of the models for Lake Taihu and their application in lake environmental management. *Ecol. Model.* **2016**, *319*, 9–20. [[CrossRef](#)]
35. Rowe, M.D.; Anderson, E.J.; Wynne, T.T.; Stumpf, R.P.; Fanslow, D.L.; Kijanka, K.; Vanderploeg, H.A.; Strickler, J.R.; Davis, T.W. Vertical distribution of buoyant *Microcystis* blooms in a Lagrangian particle tracking model for short-term forecasts in Lake Erie. *J. Geophys. Res. Oceans* **2016**, *121*, 5296–5314. [[CrossRef](#)]
36. Holtermann, P.L.; Burchard, H.; Graewe, U.; Klingbeil, K.; Umlauf, L. Deep-water dynamics and boundary mixing in a nontidal stratified basin: A modeling study of the Baltic Sea. *J. Geophys. Res. Oceans* **2014**, *119*, 1465–1487. [[CrossRef](#)]
37. Klingbeil, K.; Lemarié, F.; Debreu, L.; Burchard, H. The numerics of hydrostatic structured-grid coastal ocean models: State of the art and future perspectives. *Ocean Model.* **2018**, *125*, 80–105. [[CrossRef](#)]
38. Umlauf, L.; Lemmin, U. Interbasin exchange and mixing in the hypolimnion of a large lake: The role of long internal waves. *Limnol. Oceanogr.* **2005**, *50*, 1601–1611. [[CrossRef](#)]
39. Becherer, J.K.; Umlauf, L. Boundary mixing in lakes: 1. Modeling the effect of shear-induced convection. *J. Geophys. Res. Oceans* **2011**, *116*, C10017. [[CrossRef](#)]
40. Gräwe, U.; Holtermann, P.; Klingbeil, K.; Burchard, H. Advantages of vertically adaptive coordinates in numerical models of stratified shelf seas. *Ocean Model.* **2015**, *92*, 56–68. [[CrossRef](#)]
41. Klingbeil, K.; Burchard, H. Implementation of a direct nonhydrostatic pressure gradient discretisation into a layered ocean model. *Ocean Model.* **2013**, *65*, 64–77. [[CrossRef](#)]
42. Umlauf, L.; Burchard, H. Second-order turbulence closure models for geophysical boundary layers: A review of recent work. *Cont. Shelf Res.* **2005**, *25*, 795–827. [[CrossRef](#)]
43. Holtermann, P.; Burchard, H.; Jennerjahn, T. Hydrodynamics of the Segara Anakan lagoon. *Reg. Environ. Chang.* **2009**, *9*, 245–258. [[CrossRef](#)]
44. Skamarock, W.C.; Klemp, J.B.; Dudhia, J.; Gill, D.O.; Barker, D.M.; Wang, W.; Powers, J.G. *A Description of the Advanced Research WRF Version 2*; National Center For Atmospheric Research, Mesoscale and Microscale Meteorology Division: Boulder, CO, USA, 2005.
45. Giorgi, F.; Mearns, L.O. Approaches to the simulation of regional climate change: A review. *Rev. Geophys.* **1991**, *29*, 191–216. [[CrossRef](#)]
46. Huang, D.L.; Gao, S.B. Impact of different reanalysis data on WRF dynamical downscaling over China. *Atmos. Res.* **2018**, *200*, 25–35. [[CrossRef](#)]
47. Stehlík, J.; Bárdossy, A. Multivariate stochastic downscaling model for generating daily precipitation series based on atmospheric circulation. *J. Hydrol.* **2002**, *256*, 120–141. [[CrossRef](#)]
48. Dee, D.P.; Uppala, S.M.; Simmons, A.J.; Berrisford, P.; Poli, P.; Kobayashi, S.; Andrae, U.; Balmaseda, M.A.; Balsamo, G.; Bauer, P.; et al. The ERA-Interim reanalysis: Configuration and performance of the data assimilation system. *Q. J. R. Meteorol. Soc.* **2011**, *137*, 553–597. [[CrossRef](#)]
49. Berrisford, P.; Dee, D.P.; Poli, P.; Brugge, R.; Fielding, K.; Fuentes, M.; Källberg, P.; Kobayashi, S.; Uppala, S.M.; Simmons, A. *The ERA-Interim Archive*; ERA Report Series, No. 2; ECMWF: Reading, UK, 2011.
50. Layden, A.; MacCallum, S.N.; Merchant, C.J. Determining lake surface water temperatures worldwide using a tuned one-dimensional lake model (*Flake*, v1). *Geosci. Model Dev.* **2016**, *9*, 2167–2189. [[CrossRef](#)]
51. Schmid, M.; Lorke, A.; Wüest, A.; Halbwachs, M.; Tanyileke, G. Development and sensitivity analysis of a model for assessing stratification and safety of Lake Nyos during artificial degassing. *Ocean Dyn.* **2003**, *53*, 288–301. [[CrossRef](#)]
52. Piccolroaz, S.; Toffolon, M. Deep water renewal in Lake Baikal: A model for long-term analyses. *J. Geophys. Res. Oceans* **2013**, *118*, 6717–6733. [[CrossRef](#)]

53. Xue, P.; Schwab, D.J.; Hu, S. An investigation of the thermal response to meteorological forcing in a hydrodynamic model of Lake Superior. *J. Geophys. Res. Oceans* **2015**, *120*, 5233–5253. [[CrossRef](#)]
54. Zhang, M.; Zhang, Y.; Yang, Z.; Wei, L.; Yang, W.; Chen, C.; Kong, F. Spatial and seasonal shifts in bloom-forming cyanobacteria in Lake Chaohu: Patterns and driving factors. *Phycol. Res.* **2016**, *64*, 44–55. [[CrossRef](#)]
55. Wang, S.-R.; Meng, W.; Jin, X.-C.; Zheng, B.-H.; Zhang, L.; Xi, H.-Y. Ecological security problems of the major key lakes in China. *Environ. Earth Sci.* **2015**, *74*, 3825–3837. [[CrossRef](#)]
56. Zhang, Y.; Ma, R.; Zhang, M.; Duan, H.; Loiselle, S.; Xu, J. Fourteen-Year Record (2000–2013) of the Spatial and Temporal Dynamics of Floating Algae Blooms in Lake Chaohu, Observed from Time Series of MODIS Images. *Remote Sens.* **2015**, *7*, 10523–10542. [[CrossRef](#)]
57. Rink, K.; Chen, C.; Bilke, L.; Liao, Z.; Rinke, K.; Frassl, M.; Yue, T.; Kolditz, O. Virtual geographic environments for water pollution control. *Int. J. Digit. Earth* **2017**, *11*, 397–407. [[CrossRef](#)]
58. Le, C.; Zha, Y.; Li, Y.; Sun, D.; Lu, H.; Yin, B. Eutrophication of Lake Waters in China: Cost, Causes, and Control. *Environ. Manag.* **2010**, *45*, 662–668. [[CrossRef](#)] [[PubMed](#)]
59. Kong, X.; He, Q.; Yang, B.; He, W.; Xu, F.; Janssen, A.B.G.; Kuiper, J.J.; van Gerven, L.P.A.; Qin, N.; Jiang, Y.; et al. Hydrological regulation drives regime shifts: Evidence from paleolimnology and ecosystem modeling of a large shallow Chinese lake. *Glob. Chang. Biol.* **2017**, *23*, 737–754. [[CrossRef](#)] [[PubMed](#)]
60. Huang, J.; Yan, R.; Gao, J.; Zhang, Z.; Qi, L. Modeling the impacts of water transfer on water transport pattern in Lake Chao, China. *Ecol. Eng.* **2016**, *95*, 271–279. [[CrossRef](#)]
61. Klingbeil, K.; Mohammadi-Aragh, M.; Gräwe, U.; Burchard, H. Quantification of spurious dissipation and mixing—Discrete variance decay in a Finite-Volume framework. *Ocean Model.* **2014**, *81*, 49–64. [[CrossRef](#)]
62. Chen, Y.-Y.; Liu, Q.-Q. Numerical study of hydrodynamic process in Chaohu Lake. *J. Hydrodyn.* **2015**, *27*, 720–729. [[CrossRef](#)]
63. Idso, S.B.; Jackson, R.D. Thermal radiation from the atmosphere. *J. Geophys. Res.* **1969**, *74*, 5397–5403. [[CrossRef](#)]
64. Hipsey, M.R.; Bruce, L.C.; Hamilton, D.P. *GLM-General Lake Model: Model Overview and User Information*; The University of Western Australia: Perth, Australia, 2014.
65. Clark, N.; Eber, L.; Laurs, R.; Renner, J.; Saur, J. *Heat Exchange between Ocean and Atmosphere in the Eastern North Pacific for 1961–71*; US Department of Commerce: Washington, DC, USA, 1974.
66. Kondo, J. Air-sea bulk transfer coefficients in diabatic conditions. *Bound. Layer Meteorol.* **1975**, *9*, 91–112. [[CrossRef](#)]
67. Liu, J.; Sun, D.; Zhang, Y.; Li, Y. Pre-classification improves relationships between water clarity, light attenuation, and suspended particulates in turbid inland waters. *Hydrobiologia* **2013**, *711*, 71–86. [[CrossRef](#)]
68. Magee, N.; Wendler, G.; Curtis, J. The Urban Heat Island Effect at Fairbanks, Alaska. *Theor. Appl. Climatol.* **1999**, *64*, 39–47. [[CrossRef](#)]
69. Menne, M.J.; Durre, I.; Vose, R.S.; Gleason, B.E.; Houston, T.G. An Overview of the Global Historical Climatology Network-Daily Database. *J. Atmos. Ocean. Technol.* **2012**, *29*, 897–910. [[CrossRef](#)]
70. Kerimoglu, O.; Rinke, K. Stratification dynamics in a shallow reservoir under different hydro-meteorological scenarios and operational strategies. *Water Resour. Res.* **2013**, *49*, 7518–7527. [[CrossRef](#)]
71. Andersen, M.R.; Sand-Jensen, K.; Woolway, I.R.; Jones, I.D. Profound daily vertical stratification and mixing in a small, shallow, wind-exposed lake with submerged macrophytes. *Aquat. Sci.* **2017**, *79*, 395–406. [[CrossRef](#)]
72. Boucher, O.; Randall, D.; Artaxo, P.; Bretherton, C.; Feingold, G.; Forster, P.; Kerminen, V.-M.; Kondo, Y.; Liao, H.; Lohmann, U.; et al. Clouds and Aerosols. In *Climate Change 2013: The Physical Science Basis. Contribution of Working Group I to the Fifth Assessment Report of the Intergovernmental Panel on Climate Change*; Cambridge University Press: Cambridge, UK; New York, NY, USA, 2013.
73. Balsamo, G.; Salgado, R.; Dutra, E.; Boussetta, S.; Stockdale, T.; Potes, M. On the contribution of lakes in predicting near-surface temperature in a global weather forecasting model. *Tellus A* **2012**, *64*. [[CrossRef](#)]
74. Sivapalan, M. Prediction in ungauged basins: A grand challenge for theoretical hydrology. *Hydrol. Process.* **2003**, *17*, 3163–3170. [[CrossRef](#)]
75. Hrachowitz, M.; Savenije, H.; Blöschl, G.; McDonnell, J.; Sivapalan, M.; Pomeroy, J.; Arheimer, B.; Blume, T.; Clark, M.; Ehret, U.; et al. A decade of Predictions in Ungauged Basins (PUB)—A review. *Hydrol. Sci. J.* **2013**, *58*, 1198–1255. [[CrossRef](#)]

76. Duan, H.; Tao, M.; Loiselle, S.A.; Zhao, W.; Cao, Z.; Ma, R.; Tang, X. MODIS observations of cyanobacterial risks in a eutrophic lake: Implications for long-term safety evaluation in drinking-water source. *Water Res.* **2017**, *122*, 455–470. [[CrossRef](#)] [[PubMed](#)]
77. Shang, G.; Shang, J. Spatial and Temporal Variations of Eutrophication in Western Chaohu Lake, China. *Environ. Monit. Assess.* **2007**, *130*, 99–109. [[CrossRef](#)] [[PubMed](#)]
78. Hupfer, M.; Lewandowski, J. Oxygen Controls the Phosphorus Release from Lake Sediments—A Long-Lasting Paradigm in Limnology. *Int. Rev. Hydrobiol.* **2008**, *93*, 415–432. [[CrossRef](#)]
79. Bruggeman, J.; Bolding, K. A general framework for aquatic biogeochemical models. *Environ. Model. Softw.* **2014**, *61*, 249–265. [[CrossRef](#)]
80. R Core Team. *R: A Language and Environment for Statistical Computing*; R Foundation for Statistical Computing: Vienna, Austria, 2017. Available online: <https://www.R-project.org/> (accessed on April 2017).



© 2018 by the authors. Licensee MDPI, Basel, Switzerland. This article is an open access article distributed under the terms and conditions of the Creative Commons Attribution (CC BY) license (<http://creativecommons.org/licenses/by/4.0/>).